Ruziev and Kim *Int J Concr Struct Mater* (2023) 17:63
https://doi.org/10.1186/s40069-023-00623-2

International Journal of Concrete Structures and Materials

RESEARCH

Open Access

A Study on the Flexural Performance of Para-aramid Fiber Reinforced Concrete Beams with Recycled Coarse Aggregates

Jamshid Ruziev[1] and Woosuk Kim[2*]

Abstract

This study aims to investigate the effectiveness of para-aramid fiber sheet in enhancing the flexural performance of reinforced concrete (RC) beams made with Environmental-Friendly Recycled Coarse Aggregates. The experimental program examines the effect of substitution ratio of recycled aggregates (0%, 30%, and 50%), type of para-aramid fiber sheet (KN 206 RFL and KN AA070-RFL), and the method of fiber sheet attachment (bottom and bottom-side). The test results show that the ultimate load-carrying capacity of RC beams reinforced with para-aramid fiber sheet attached to the bottom and side parts increased by 23.9% compared to the unreinforced specimens. The main findings of the study include the identification of the BU-type attachment method as the most effective method for enhancing the flexural performance of reinforced concrete beams. The comparison of the experimental results with analytical predictions showed that the nominal flexural strength obtained from the experimental study was lower than the analytical predictions, but the ductile capacity of the specimens indicated the effectiveness of para-aramid fiber sheet reinforcement in EFRCA RC beams for flexural strength. The study highlights the potential of using para-aramid fiber sheet in improving the flexural behavior of RC beams made with recycled aggregates, offering a sustainable solution for the construction industry.

Keywords Fiber reinforced polymer, Para-aramid fiber sheet, Recycled coarse aggregates, Flexural performance

1 Introduction

The use of fiber-reinforced polymers (FRP) for the rehabilitation and strengthening of concrete structures has been widely investigated due to their excellent mechanical properties and durability. Among various types of FRP, aramid fiber sheets have been gaining attention for their high tensile strength, toughness, and fire resistance. Aramid fiber-reinforced polymers (AFRP) are a type of composite material that have been increasingly used in concrete structures in recent years. AFRPs are made from aramid fibers, which have high strength and stiffness, and a polymer matrix, which provides toughness and durability. AFRPs have several advantages over other types of reinforcement materials, including high strength-to-weight ratio, corrosion resistance, and ease of installation. They are also non-magnetic, non-conductive, and have low thermal expansion, which makes them suitable for use in sensitive environments such as Magnetic Resonance Imaging (MRI) rooms and nuclear power plants. Several studies have investigated the use of AFRPs in concrete structures, including beams, columns, and slabs. In general, the results have shown that AFRPs can provide significant improvements in strength and ductility compared to unreinforced concrete, and in

Journal information: ISSN 1976-0485 / eISSN 2234-1315.

*Correspondence:
Woosuk Kim
kimw@kumoh.ac.kr
[1] Department of Architectural Engineering, Kumoh National Institute of Technology, Gumi 39177, Republic of Korea
[2] Department of Architectural Engineering, Kumoh National Institute of Technology, 61 Daehak-Ro, Gumi, Gyeongsangbuk-Do 39177, Republic of Korea

some cases can even exceed the performance of traditional steel reinforcement.

Domestic research studies have shown promising results in the use of AFRPs for the improvement of the mechanical properties and durability of concrete structures. The paper by Cho et al. (2016) focuses on evaluating the use of aramid fiber sheet (AFS) as a reinforcement material in sustainable structural concrete. The study involved the use of recycled aggregates (RA) in combination with AFS to produce concrete samples for testing. The compressive strength, tensile strength, and flexural strength of the concrete samples were then tested. The results showed that the addition of AFS improved the tensile and flexural strength of the concrete, particularly at higher AFS content levels. The authors concluded that the use of AFS in combination with RA can result in sustainable structural concrete with improved mechanical properties. The study highlights the potential for the use of AFS as a reinforcement material in sustainable concrete applications. According to Kim et al. (2012), the study focuses on the experimental study of the effects of beam sizes and CFRP (carbon fiber reinforced polymers) layers on the structural behavior of reinforced concrete beams that were strengthened using CFRPs. The study aimed to evaluate the effect of different variables such as the number of CFRP layers, beam sizes, and the placement of the CFRP layers on the behavior of the strengthened beams. The study applied the CFRP sheets in various configurations, including one layer, two layers, and three layers, and evaluated the effect of each configuration on the load-carrying capacity and deflection of the beams. The results showed that the application of CFRP sheets increased the load-carrying capacity and ductility of the strengthened beams. The study also found that the beam size had a significant effect on the load-carrying capacity and the amount of deflection. Specifically, the larger beams showed a higher load-carrying capacity than the smaller beams. The study suggests that the use of CFRP sheets is an effective method to improve the load-carrying capacity and ductility of reinforced concrete beams. In Kim et al. (2014), the flexural strengthening effect of recycled coarse aggregate (RCA) reinforced concrete (RC) beams using carbon fiber reinforced polymers (CFRPs) was investigated. CFRP sheets with different widths and layers were used to strengthen the beams. The test results showed that the ultimate load-carrying capacity, flexural strength, and stiffness of the RCA RC beams were improved by CFRP strengthening. The use of wider and more layers of CFRP sheets led to a higher improvement in the structural performance of the RCA RC beams. The authors concluded that the use of CFRP sheets is an effective method to enhance the flexural performance of RCA RC beams, and the strengthening effect depends on the width and layers of the CFRP sheets.

Table 1 presents the results of above research studies on fiber reinforced concrete [(1) Cho et al. 2016, (2) Kim et al. 2012, (3) Kim et al. 2014]. Results of the studies show 38%, 39.9% and 100.8% increase in maximum load resistance. By the study of (1) Cho Y.S. et al. (2016) the

Table 1 Previous domestic research test results for strength of fiber reinforced concrete

Classification	Fiber reinforcement material				At maximum resistance	
	Type of fiber reinforcement material	Tensile strength (GPa)	Modulus of elasticity (GPa)	Applying method	Load (kN)	Displace ment (mm)
(1) Cho. et al. (2016)	Aramid fiber sheet	2.1	117.7	-	62.9	51.4
				B*	88.1	49.2
				BU*	86.9	35.6
				BS*	131.9	33.1
(2) Kim. et al. (2012)	CFRP* sheet	4.5	245.2	M2*	99	21.9
				M3	95	17.5
				M4	84.4	14.4
				L3*	169.4	30.3
(3) Kim et al (2014)	CFRP sheet	3.5	235	R15-CFS	81.1	32.6
				R30-CFS	78.3	51.2
				R50-CFS	71.1	43.2
	CFRP plate	3.5	165	R30-CFP	97.9	18.2
				R50-CFP	103.2	52.3

CFRP Carbon Fiber Reinforcement Polymer, *B* application to the bottom part of beam, *BU* application to the bottom and side part of beam, *BS* application to the bottom part and U-band both ends, *M2* medium size (3200 × 150x250 mm) of reinforced beam with 2 layers of reinforcement sheet, *L2* large size (4600 × 300x350 mm) of reinforced beam with 2 layers of reinforcement sheet ductility ratio increased by 2.75 ~ 6.2. According to (2) Kim et al. 2012, the load capacity of specimens increased, however, the failing is occurred after carbon fiber reinforcement polymers starts debonding. For (3) Kim et al. 2014, the ultimate loads increased by an average 32.5% for the beams reinforced with CFRP sheets and by an average 79% for ones reinforced with CFRP plates. Also, there was an increase in ductility by 121% and 109% for CFRP sheet and plate reinforced specimens, respectively.

Overseas researchers have also evaluated the feasibility of using fiber-reinforced polymers as a sustainable alternative to traditional strengthening materials in concrete structures. The study by Attari et al. (2012) investigated the flexural strengthening of concrete beams using different types of fiber-reinforced polymer (FRP) sheets. Three types of FRP sheets were used, including carbon FRP (CFRP), glass FRP (GFRP), and a hybrid of CFRP and GFRP. The study involved testing 18 concrete beams, with six beams for each type of FRP sheet. The beams were tested under four-point bending to evaluate their flexural strength, stiffness, and cracking behavior. The results showed that all types of FRP sheets significantly improved the flexural performance of the concrete beams, with CFRP being the most effective. The hybrid CFRP/GFRP sheets also showed promising results, with a performance that was between those of the individual CFRP and GFRP sheets. The study concluded that the use of FRP sheets can be an effective method for flexural strengthening of concrete beams. In M. Garcez et al. (2008), the structural performance of reinforced concrete beams strengthened with different types of FRP systems, including aramid fiber-reinforced polymers, was investigated. The test setup included four-point bending tests, and the test parameters included the number of layers of FRP, the type of FRP, and the level of prestressing. The results showed that the aramid fiber-reinforced polymer provided higher stiffness and load-carrying capacity compared to glass fiber-reinforced polymer, and similar performance to carbon fiber-reinforced polymer. The authors concluded that aramid fiber-reinforced polymers could be a viable option for strengthening reinforced concrete beams. Looking at the results, there were increases by 83.3%, 59.4%, and 77.9% for CFB_02, AFB_02 and GFB_02, respectively (Table 2).

The significance of our research lies in the investigation of the effectiveness of using para-aramid fiber sheets for strengthening recycled aggregate concrete (RAC) beams. RAC is a sustainable alternative to traditional concrete, but its mechanical properties are generally lower than those of conventional concrete Arezoumandi et al. (2015). Therefore, enhancing the performance of RAC beams using cost-effective and sustainable materials such as para-aramid fibers is essential Tatar and Milev (2021), Biswas et al. (2023). This study adds to the existing literature by providing new insights into the effectiveness of para-aramid fiber sheets in enhancing the flexural behavior of RAC beams. To the best of our knowledge, there are limited studies that have investigated the use of para-aramid fibers in RAC beams. This study also contributes to the literature by exploring the effects of different parameters such as the attachment method and replacement ratio of recycled aggregates on the flexural behavior of RAC beams reinforced with para-aramid fiber sheets. Furthermore, the use of para-aramid

Table 2 Previous foreign research test results for strength of fiber reinforced concrete

Classification	Fiber reinforcement material				Load values (kN)		
	Type of fiber reinforcement material	Tensile strength (MPa)	Modulus of elasticity (GPa)	Applying method	Cracking	Yield	Ultimate
(1) Attari et al. (2012)	CFRP	403	43.5	PA1*	10.7	43.6	77.8
	GFRP*	325	19.2	PA2*	12.4	45.8	78.9
				PA3*	11.1	43.6	86.5
	Hybrid (Twin) CFRP + GFRP	400	28	PB4*	10.1	41.7	76.6
				PB5*	9.3	43.3	68.2
	Hybrid fabric HFRP	218	27	PB6*	7.2	41.2	54.9
(2) Garcez et al. (2008)	CFRP	3400	227	CFB_01*	20.6	83.8	128.7
				CFB_02	25.7	88.5	189.1
	AFRP	2800	124	AFB_01*	20.6	83.8	134.5
				AFB_02	25.2	88.9	164.5
	GFRP	1517	72.4	GFB_02*	29.8	88.9	183.5

GFRP Glass Fiber Reinforcement Polymer, *PA1* CRFP wrap 1 layer 0° and 1 layer 90°U shape, *PA2* GFRP wrap 2 layers at 0° and 1 layer 90°U shape, *PA3* 1 layer GFRP 0° 1 layer CFRP 0°U shape, *PB4* 3 layers HFRP U shape, *PB5* 2 layers HFRP U shape, *PB6* 3 layers HFRP, *CFB_01* 1 layer of CFRP reinforcement, *AFB_01* 1 layer of Aramid FRP reinforcement, *GFB_02* 2 layers of GFRP reinforcement fibers is an expensive approach, but it provides numerous advantages such as high tensile strength, durability, and resistance to environmental degradation. Therefore, it is essential to explore its effectiveness in enhancing the performance of sustainable concrete such as RAC. This research investigates a new approach for enhancing the mechanical properties of RAC beams using para-aramid fibers. Our study contributes to the literature by providing new insights into the effectiveness of para-aramid fiber sheets in enhancing the flexural behavior of RAC beams and exploring the effects of different parameters on their performance.

2 Experimental Method

The experimental method used in this study aimed to investigate the flexural performance of recycled aggregate RC beams reinforced with para-aramid fiber sheets. To achieve this, three types of reinforced beams using para-aramid fiber sheets were produced, and three types of recycled aggregate RC beam specimens without para-aramid fiber sheets were also created. The flexural performance of each specimen type was evaluated, and the differences were analyzed to determine the effects of para-aramid fiber sheet reinforcement.

A total of 16 RC beams were produced, using recycled coarse aggregates (RCA) Rao et al. (2007), and evaluated for their flexural characteristics. Three types of environmentally friendly recycled coarse aggregates (EFRCA) volume fractions (0%, 30%, and 50%) were used to investigate their effects on the flexural behavior of the para-aramid fiber sheet RC beams. Two types of para-aramid fiber sheets with main parameters of 4.5 mm and 14 mm intervals were also selected and applied to the bottom and side parts of the specimens.

Prior to conducting the experiment, the study direction and purpose were established by analyzing existing research and cases. The experiment objective was then defined, and the experiment was planned by setting up experiment factors, organizing specimens, and measuring the flexural performances. After conducting the experiment, the results, including load–displacement data, failure shape, and other relevant information, were analyzed to identify the flexural characteristics of the para-aramid fiber sheet RC beams. The results indicated that partially replacing natural aggregates with EFRCA could increase the durability of the concrete produced. Additionally, the potency of the reinforced beam experiment was verified by comparing the results of the flexural performance experiment with theoretical analysis results.

2.1 Material and Mixture Properties

The experimental study involved the preparation of specimens using different types of materials such as environmentally friendly recycled coarse aggregates Ahmadi et al. (2017), natural aggregates, para-aramid fiber sheets, and Portland cement. Fine river sands with a diameter of less than 0.5 mm were used as fine aggregates and natural coarse aggregates with a maximum size of up to 11 mm were used. Table 3 presents the material properties of the aggregates used in the study, including fineness modulus (FM), specific gravity (SG), absorption rate of aggregate (ARA), and maximum size of materials.

Para-aramid fiber sheets were used as a reinforcing fiber in composite materials due to their high strength, elastic modulus, lightweight, and impact resistance properties Lee et al. (2018), Almusallam (2006). Table 4 shows the material properties of para-aramid fiber used in the study, including tensile strength, thickness, elastic modulus, weight per unit area, and elongation.

Table 5 provides information on the material properties of the Portland cement used in the production of specimens in the study. The table includes the percentages of various chemical compounds present in the cement, such as SiO2, Al2O3, Fe2O3, MgO, CaO, and SO3. The specific gravity of the cement and its fineness, measured in cm2/g, are also provided. The cement used in the study

Table 4 Material properties of para-aramid fiber

Type	Tensile strength (MPa)	Thickness (mm)	Elastic modulus (GPa)	Weight per unit area (g/m^2)	Elongation
Aramid fiber	2400	0.21	113.7	300	1.44

Table 3 Material properties of aggregates

Aggregate Types		FM (%)	SG (g/cm^3)	ARA (%)	Wear Rate (%)	Maximum Size (mm)
Fine aggregate		2.2	2.6	1.5		
Coarse aggregate	NA	6.8	2.6	1.1	21.1	11
	RA	6.4	2.5	2.8	34.2	19

FM Fineness modulus (the coarseness or fineness measurement of a given aggregate), *SG* Specific gravity (ratio of the density of a given solid to the density of water), *ARA* Absorption rate of aggregate (rate of moisture absorption into the aggregates)

Table 5 Material properties of cement

SiO2 (%)	Al_2O_3 (%)	Fe_2O_3 (%)	MgO (%)	CaO (%)	SO_3 (%)	Specific gravity	Fineness (cm^2/g)
22.4	6.2	2.9	3.2	62.1	2.3	3.15	3200

Table 6 Concrete mixing ratio according to EFRCA ratio

Classifi cation	Weight(kg/m^3)					
	Water	Cement	Fine aggregate	Natural aggregate	Recycled aggregate	Water reducing admixture
R0	171.1	380.1	770.5	974.6	0	3.8
R30				713.2	261.4	
R50				487.2	487.2	

Table 7 Concrete strength properties according to EFRCA ratio

Classification	R0	R30	R50
Concrete compressive strength (MPa)	49	48.6	47.5

had w/C ratio of 45%, 24 MPa compressive strength, specific gravity of 3.15 and a fineness of 3200 cm2/g.

In this study, RCA was used as a partial replacement for natural coarse aggregates in the concrete mixtures. To ensure the quality and workability of the concrete mixture, the absorbed water by RCA was taken into account during the mix design process. The water absorption of RCA was measured prior to use and the amount of water in the mix design was adjusted accordingly.

Table 6 shows the concrete mixing ratio according to the EFRCA (Environmentally Friendly Recycled Coarse Aggregates) ratio. The table presents the weight of the various components used in the concrete mix, which includes water, cement, fine aggregate, natural aggregate, recycled aggregate, and water-reducing admixture.

The mix design was conducted following the guidelines of the American Concrete Institute (ACI) method ACI Committee 318, (2008). Table 7 is divided into three classifications, R0, R30, and R50, which represent the amount of recycled aggregate used in the mix. R0 indicates that no recycled aggregate was used, while R30 and R50 indicate that 30% and 50% of the natural coarse aggregates were replaced with recycled aggregates, respectively. Strength properties of concrete according to recycled aggregates used by being substituted by 0%, 30%, and 50% based on Table 7, and mix proportion table is as shown in Table 6.

Regarding the identification of the beam specimens, F10, F13, and F16 correspond to the beam tensile rebar size (in mm), and the number after the letter indicates the percentage of recycled aggregates used in the concrete mix. For instance, F10R30-N refers to the beam with a tensile rebar size of 10 mm and 30% of the recycled aggregate in the concrete mix, which was reinforced with the traditional method without para-aramid fibers.

2.2 Specimen Design

The design and production of the 16 beams for the structural tests involved various stages. The beams were designed with a length of 2560 mm, width of 135 mm, height of 270 mm, and an effective depth of 232 mm. The center-to-center span was 2260 mm, and all beams had a (a/d) ratio greater than 2, in accordance with beam theory. Three types of deformed rebars, D10, D13, and D16, were used as tensile rebars, and D10 stirrups were placed at every 100 mm interval, as illustrated in Fig. 1.

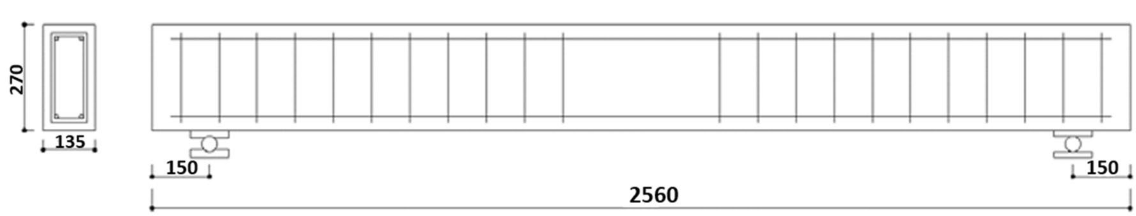

Fig. 1 Design of test specimen

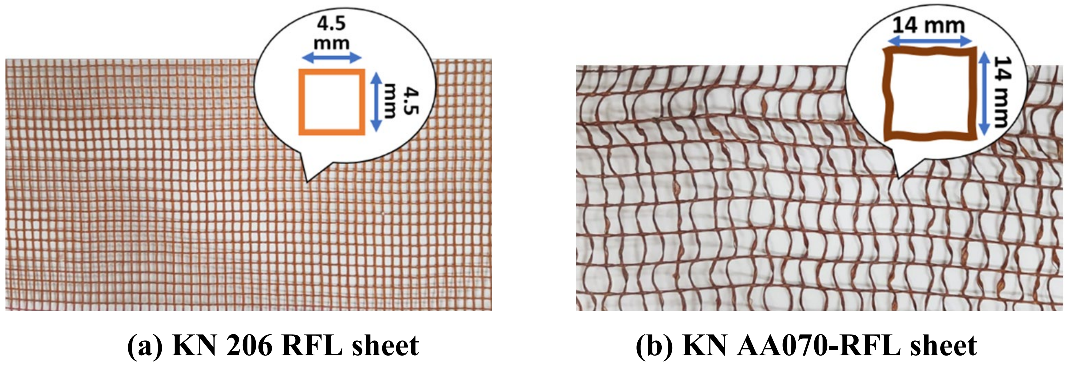

Fig. 2 Para-aramid fiber sheet

The production process was carried out at the structural engineering laboratory of Kumoh National Institute of Technology. Initially, cement was mixed with sand using a special mixer machine, and coarse aggregates were added to the mixture in the mixing drum. Water was gradually poured into the mixture until it achieved a uniform consistency. In some cases, a high-range water reducer was added to achieve the desired workability. After casting, all specimens were moist-cured for 7 days and then air-cured after beams were demolished. The curing process continued for a total of 28 days Etxeberria et al. (2007).

Following the curing period, the RC beams were dried for 4 days to prepare for attaching para-aramid fiber sheets. The first step involved concrete face treatment, whereby the surface of the beams was ground down using a grinder. Next, a primer was applied onto the washed and dried surface by applying an infiltrative hardening agent before attaching the fiber sheet. The final step involved adhering the aramid fiber sheet using epoxy adhesion Kim J. et al. (2012), Kim et al. (2020). After the completion of the fiber sheet attachment operation, the specimens were cured for 7 days until the flexure test was conducted.

To evaluate the flexural performance of reinforcement material, two type of para-aramid sheets (KN 206 RFL and KN AA070-RFL), as shown in Fig. 2, were applied to the bottom of beam (B2-type), the bottom-side part of beam (BU-type), and the bottom part of beam (LB2-type). For B2-type of application, the para-aramid fiber sheet with 4.5 mm interval (KN 206 RFL) as shown in Fig. 3a, was attached in two layers onto the bottom part of beam. With the same method of applying, but instead of 4.5 mm interval aramid fiber sheet, 14 mm interval of it (KN AA070-RFL) as shown in Fig. 3b, was used for LB2-type of application. In the BU-type application, both type of fiber sheets were used. First, the fiber sheet with short interval was attached onto the bottom part of beam. After epoxy adhesion, secondly, the fiber sheet of long interval was attached onto the bottom part and both side parts of beam Lee et al. (1998).

2.3 Test Equipment

Sixteen produced beam specimens were tested using the Actuator installed on the reaction wall. This machine has a capacity 980 kN on the frame. The beams were simply supported with one end hinged condition and the other on roller support at Architectural Engineering Laboratory Building of Kumoh National Institute of Technology as shown in Fig. 4. The test span was kept as 2260 mm. Two-point loads were applied transversely at 400 mm apart at about the center Kim W. (2011).

To measure beam deflections and cracks width, the specimens had multiple Linear Variable Differential Transducer (LVDT) mounted on the middle range of the beam. The load was applied from the spreader to the upper surface of the beam and the steel bearing plates were placed at the loading and support points to prevent local crushing of the concrete. Measurements were collected through a computer-controlled data and in each loading step crack width was measured from time to time using an eye gauge with a lower resolution of 0.01 mm. Steel strain gauge was attached at the bottom of the reinforcement steel. Three concrete strain gauges were attached in a vertical orientation at the center line (Fig. 5).

In total, sixteen specimens were tested, each using recycled aggregates and para-aramid fiber sheets, and their flexural characteristics were analyzed using the experimental data collected.

3 Experimental results

3.1 Crack-Pattern and Failure Modes

During the testing process, crack development was carefully monitored using a crack width gauge, and the crack patterns were recorded on the beams at each load

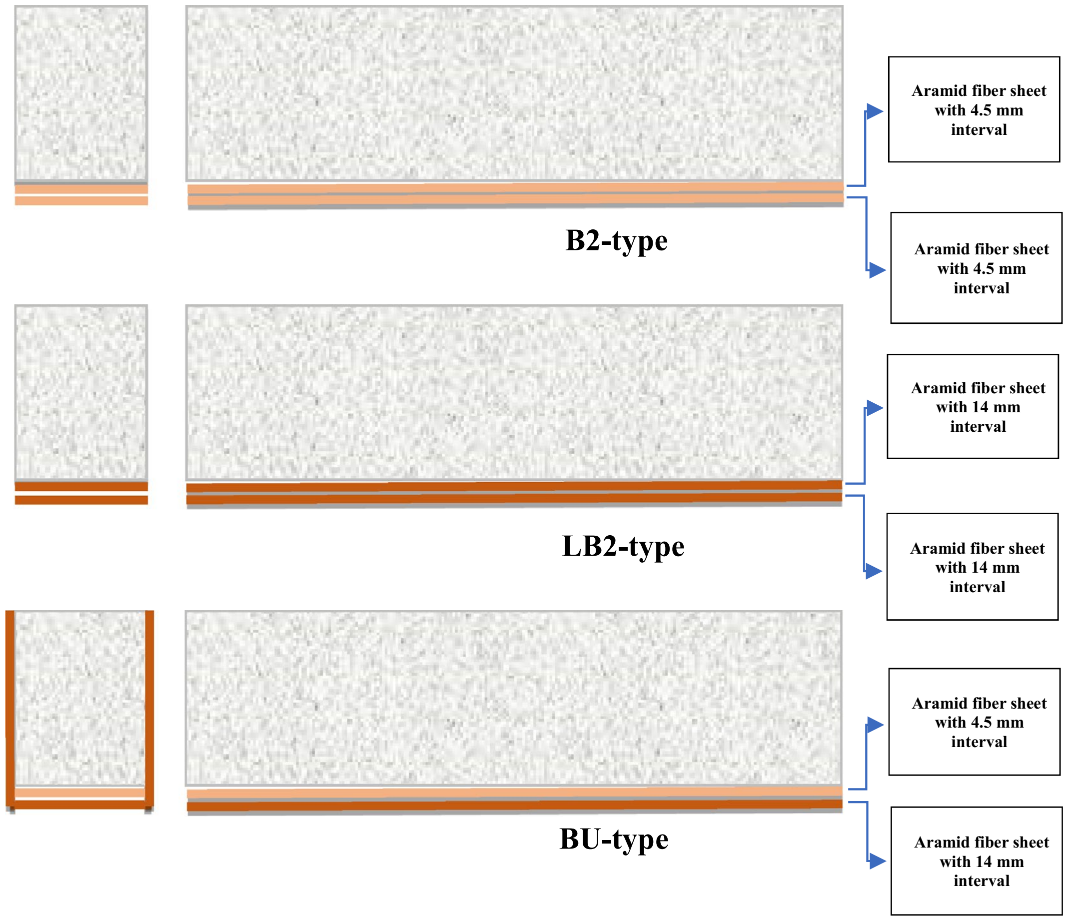

Fig. 3 Type of RC beam according to para-aramid fiber sheet

increment using colored markers. The specimens were closely observed for any signs of premature failure. The crack patterns and failure modes of the specimens are shown in the accompanying figures. It is apparent from the results that the main areas for flexural and diagonal cracking were over the constant moment area and the shear span section, which is in the middle of the loading point and the support. The level of cracking and crack width varied depending on the type of para-aramid fiber sheet application, indicating the influence of para-aramid fiber sheet on the flexural behavior of EFRCA RC beam.

3.1.1 Evaluation of Crack Pattern Properties for non-Fiber Reinforcement Specimens

The crack patterns and failure modes of five non-reinforced specimens are presented in the figures below (Fig. 6). These specimens failed due to a lack of support and exhibited flexural failure. The initial cracks appeared before reaching a load value of 17–28 kN, respectively. Generally, the cracks were generated vertically at the mid-span. As the load was further increased Guo et al. (2022), small hairline cracks appeared on the beams, and the number of these cracks increased near the supports with the gradual increase of the load until failure occurred. Among the non-reinforced N-series specimens, F10R30-N showed better ductile behavior at a lower level of reinforcement, resulting in a more ductile failure mode. F16R30-N, on the other hand, had a higher level of reinforcement and could carry a higher load before reaching its peak moment carrying capacity Ortiz et al. (2023). However, it still failed at a relatively low load level compared to specimens reinforced with para-aramid fiber sheets. This emphasizes the need for proper reinforcement techniques to improve the flexural behavior and overall structural performance of reinforced concrete beams.

3.1.2 Evaluation of Crack Pattern Properties for B2/LB2-type Fiber Reinforcement Specimens

Fig 7 shows the fracture behavior of six specimens reinforced with recycled coarse aggregates and B2- and

Fig. 4 Test set-up

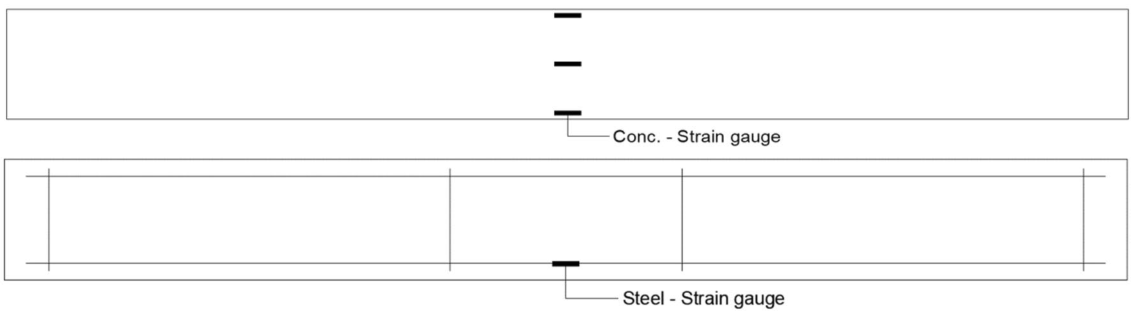

Fig. 5 Strain gauges setting up

LB2-type of aramid fiber sheet attachment method. Hairline cracks were observed prior to reaching value of 17–28 kN, respectively, which was similar to N-series of specimens. With further increases in load, the cracks further widened and became more prominent. The cracks initially generated at mid span of the beam and initial lateral crack occurred at diagonal tension bar. As the load increased, diagonal tension bar crack progressed from member bottom part toward actuating point, as the bending crack at the center part of the beam moves on, the width further increased. In the case of F16R30-LB2 specimen, initial cracks were observed prior to reaching a value of 28.2 kN and the failure behavior of this beam specimen at the peak moment capacity of 115.3 kN and a deflection value of 84.5 mm is shown in Fig. 7e. After the peak moment capacity of 115.3 kN, the beam started losing its capacity and load values decreased, with a significant increase in the deformation capacity of the beam. Excepting the specimen of F16R30-LB2, all other B2-type fiber reinforcement specimens faced to tensile failure.

3.1.3 Evaluation of Crack Pattern Properties for BU-type Fiber Reinforcement Specimens

The graphical and experimental failure patterns of BU-type aramid fiber sheet attachment series of five specimens are shown in Fig. 8. In BU-series of the beams, the value of flexural reinforcement was considerably higher compared to N- and B2/LB2-series of specimens. Fig 8 presents the graphical and experimental cracking patterns of BU-type serial specimens at different ratio of recycled aggregates. Appearing of cracks in this type of specimens decreased 3–4 times comparing with other types of specimens. Furthermore, BU-type specimens showed significant increase in flexural reinforcement with the highest results of 117.8 kN moment capacity (F16R30-BU) and 81.4 mm of ultimate displacement (F10R30-BU) in this experimental study. In the case of BU-series of specimens, diagonal hairline crack forms were spotted near the loading points of specimens. It can be clearly seen that bridging effect of the BU-type fiber reinforcement beams was more effective than type of

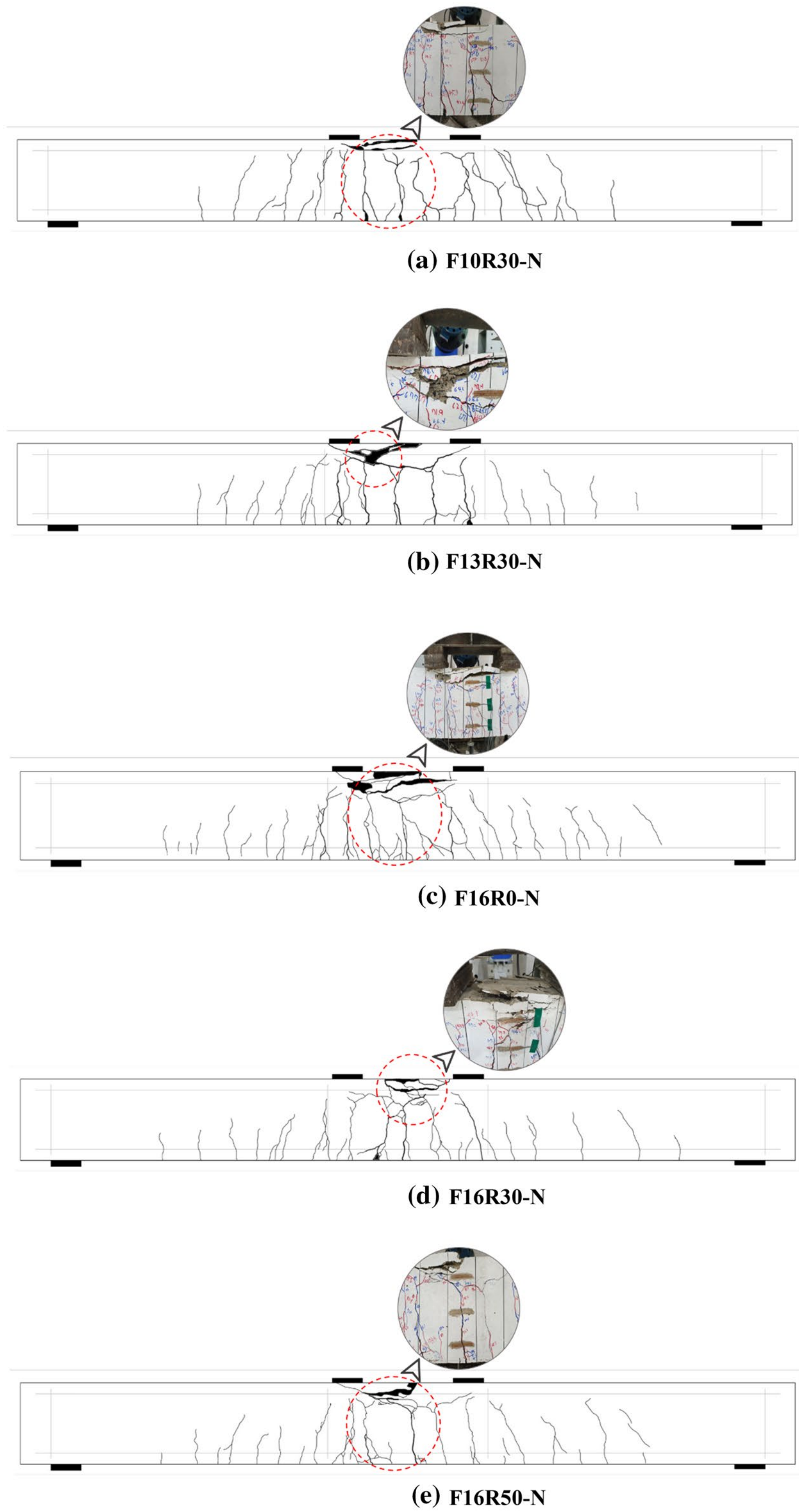

Fig. 6 Schematics of sequential crack patterns of non-fiber reinforcement specimens (N-series)

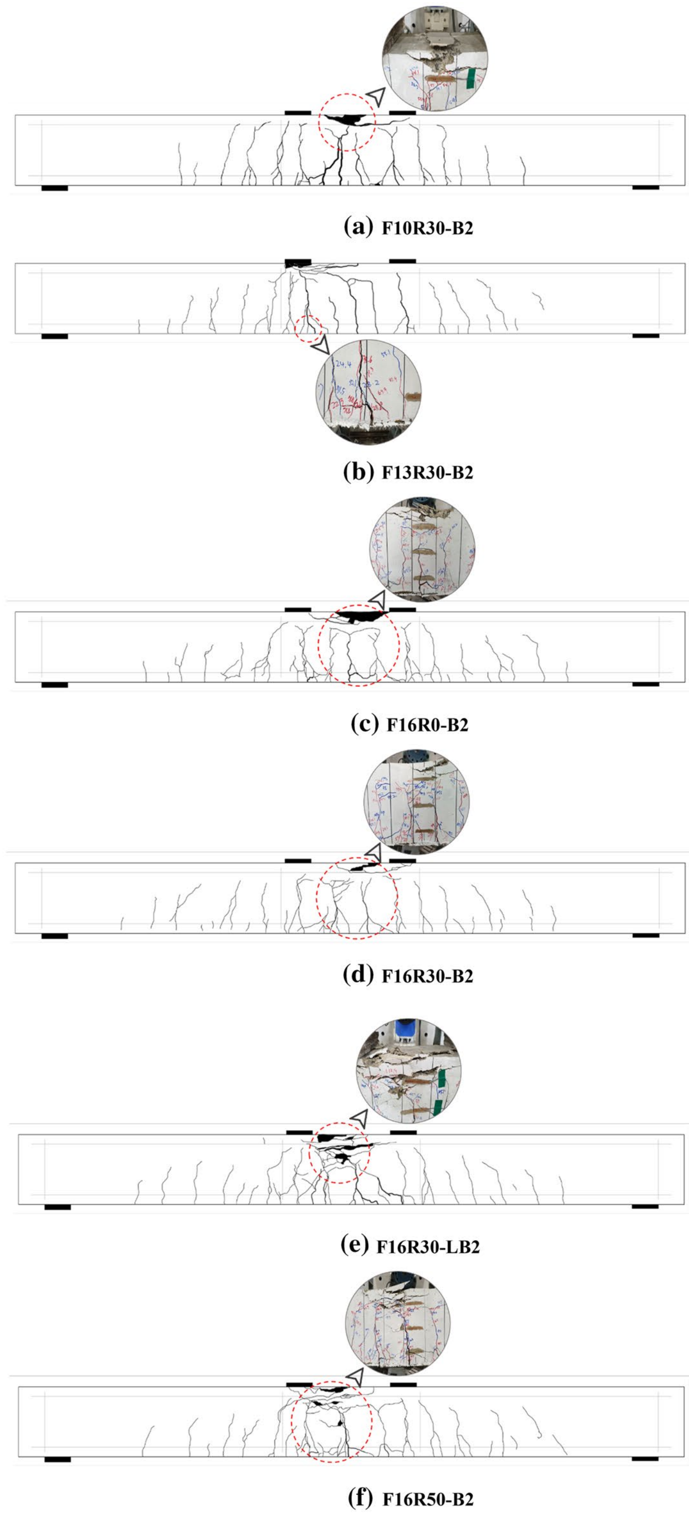

Fig. 7 Schematics of sequential crack patterns of B2/LB2-type fiber reinforcement specimens (B2/LB2-series)

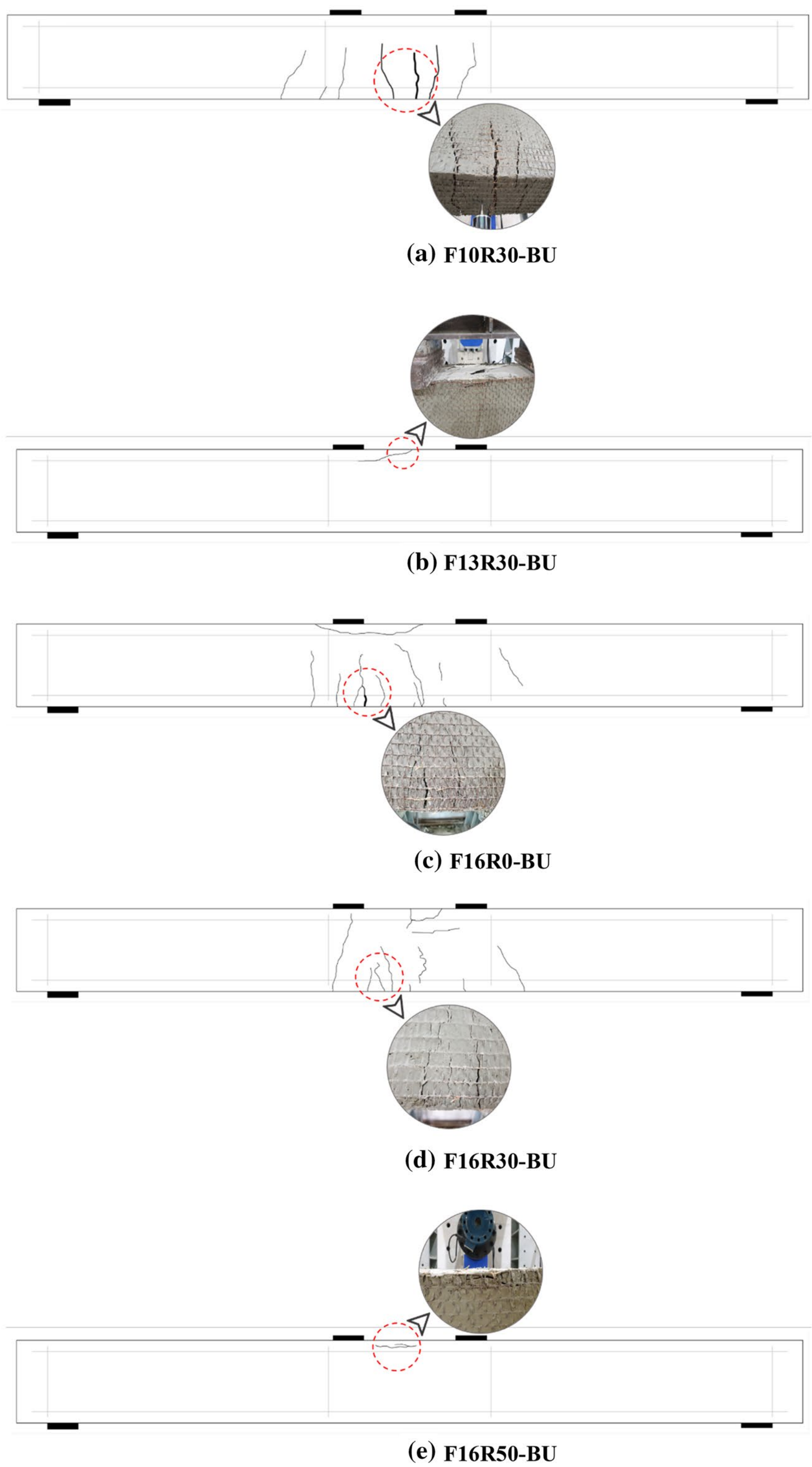

Fig. 8 Schematics of sequential crack patterns of BU-type fiber reinforcement specimens (BU-series)

Table 8 Test results and failure mode flexural beam specimen

Specimen	Initial cracking load (kN)	Peak load (kN)	Rate of increase and decrease (%)	Ultimate displacement (mm)	Failure mode
F10R30-N	21	56	–	80.6	Flexural
F10R30-B2	22	58.7	4.8	66.1	Tensile
F10R30-BU	37.4	69.4	23.9	81.4	Flexural
F13R30-N	28.7	79	–	69.8	Flexural
F13R30-B2	26.8	75.6	− 4.4	54.5	Tensile
F13R30-BU	40.9	81.5	3.1	67.4	Flexural
F16R0-N	17.3	108.2	–	54.9	Flexural
F16R0-B2	17.6	108.4	0.3	44.1	Tensile
F16R0-BU	21.1	115.4	6.7	73.2	Flexural
F16R30-N	27.4	111.5	–	69.5	Flexural
F16R30-B2	28.5	108.5	− 2.7	40.6	Tensile
F16R30-BU	34.9	117.8	5.7	68.9	Flexural
F16R30-LB2	28.2	115.3	3.4	84.5	Flexural
F16R50-N	26.8	108.8	–	48.1	Flexural
F16R50-B2	26.1	112.7	3.6	68	Tensile
F16R50-BU	29.2	112.3	3.2	42.6	Flexural

specimens. The influence of the external strengthening type of BU-series was found to be significant. It can be clearly seen that the cracks are retarded by the presence of BU-type of fiber sheet reinforcement comparing the crack patterns of BU-series and other series of RC beams.

3.2 Flexural Test Results

In this study, the flexural strength of sixteen RC beams was found to be various due to the para-aramid fiber sheet attachment method. Among the N-series specimens, beam F10R30-N exhibited better ductile behavior than the others at the peak displacement level of 80.6 mm. The F10R30-N specimen had a lower level of reinforcement compared to the other specimens. This lower level of reinforcement may have resulted in a more ductile failure mode Bai and Sun, (2010), Kim and Kwak, (2015). On the other hand, specimen F16R30-N exhibited failure behavior at the peak moment carrying capacity of a 111.5 kN load (Table 8). The F16R30-N specimen had a higher level of reinforcement compared to the other non-reinforced specimens, as it contained a larger tensile rebar, F16. The increased level of reinforcement allowed the specimen to carry a higher load before reaching its peak moment carrying capacity Sato et al. (2007), Yang and Jeong (2016). However, despite having a higher peak moment carrying capacity, the specimen still failed at a relatively low load level compared to the specimens reinforced with para-aramid fiber sheets. This highlights the importance of using appropriate reinforcement techniques to enhance the flexural behavior and overall structural performance of reinforced concrete beams Yoo et al. (2020).

Also, F16R30-LB2 specimen showed almost the same first crack load in 28.2 kN comparing to the reference control beam F16R30-N specimen. Otherwise, EFRCA reinforcement concrete beams reinforced with para-aramid fiber sheet in the bottom and two sides provided an effective enhancement with an improvement of initial crack load capacity.

The BU-type attachment method of para-aramid fiber sheet for strengthening reinforced concrete beams was found to be very efficient based on the experimental results. The enhancement mechanism or action mechanism of this type is related to the even distribution of load across the surface of the concrete beam. During the application of the BU-type aramid fiber sheet attachment method, the adhesive material is evenly spread over the surface of the beam. This leads to a more uniform distribution of the load on the surface of the beam, which results in a reduction in the number of cracks compared to other types of reinforcement methods. Moreover, the BU-type attachment method provides a more effective bonding between the aramid fiber sheet and the concrete surface, resulting in a higher resistance to cracking and a more efficient transfer of stress Saleem et al. (2019). The evenly distributed load, combined with the high bonding strength, provides an improved load-carrying capacity and a better flexural behavior of the reinforced concrete beams. Therefore, it can be concluded that the BU-type attachment method is the most effective way for

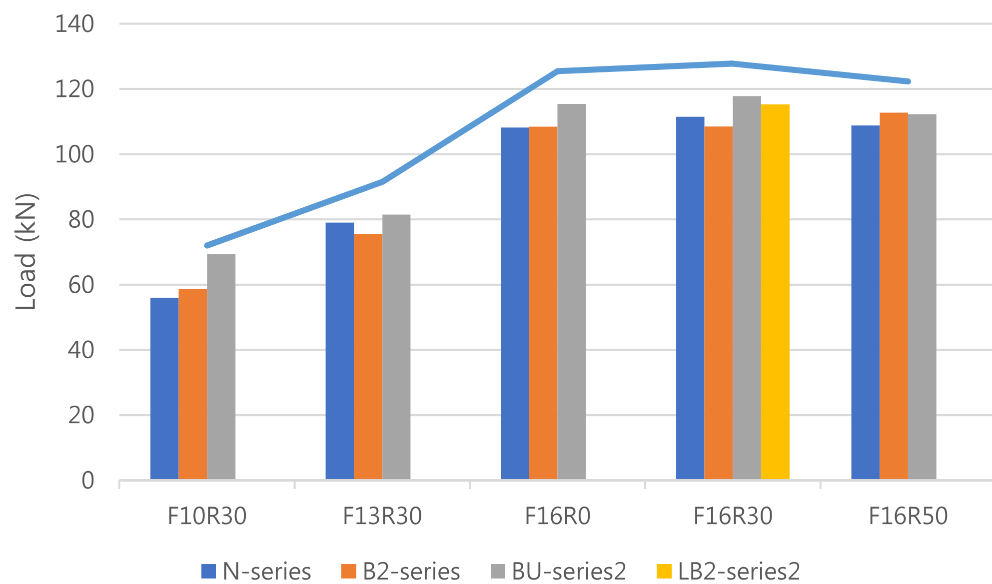

Fig. 9 The ultimate load of test specimens

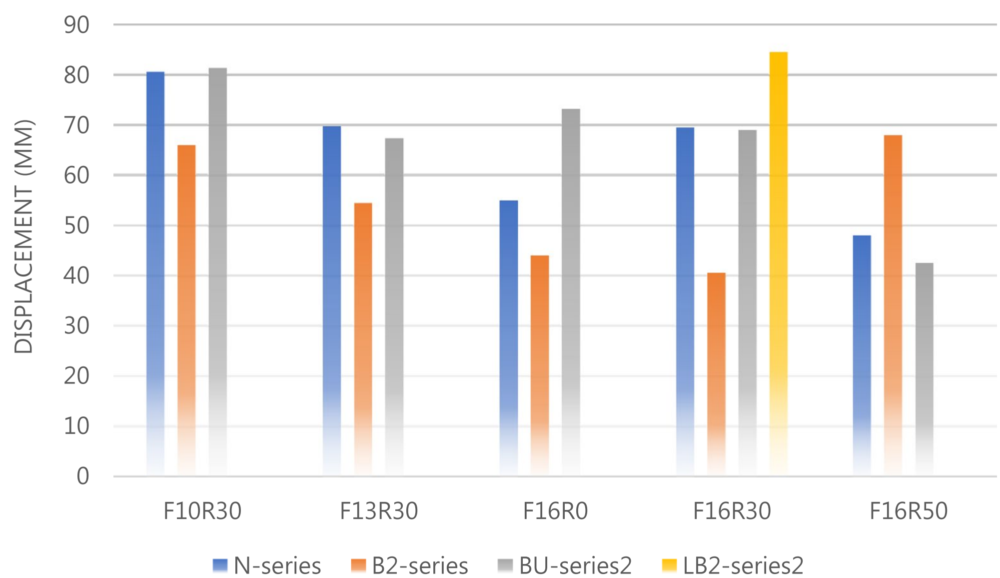

Fig. 10 Ductility of test specimens

strengthening reinforced concrete beams due to its ability to evenly distribute the load and provide a strong bond between the aramid fiber sheet and the concrete surface.

The flexural test results revealed that the aramid fiber sheet used for the reinforcement of the B2-series specimens, as depicted in Fig. 2a, exhibited a behavior that could not be sustained beyond a certain load. Tensile failure mode occurred by being broken of aramid fiber sheet. It was confirmed that there is little strength enhancing effect compared to the test specimens without fiber reinforcement (Fig. 9).

In the case of BU-series specimens, the sheet used for reinforcing LB2-series specimens (Fig. 2b) was applied one layer to bottom and side section. Consequently, it was confirmed that the flexural strength was improved by increasing the load rate of 3.1% to 23.9% as shown in Table 8. In addition, it could be seen that the strength-improving effect was more pronounced in the specimens with a lower tensile reinforcing ratio among the reinforced specimens and showed more ductile behavior Qureshi (2022), Lu et al. (2021).

Table 9 A comparison of test results with existing structural analysis methods

Specimens	$M_{n, exp}$ (kN*m)	$M_{n, El\text{-}Mihilmy}$ (kN*m)	$M_{n, ACI\ 440.2R\text{-}08}$ (kN*m)	$M_{n, exp}/M_{n, El\text{-}Mihilmy}$	$M_{n, exp}/M_{n, ACI\ 440.2R\text{-}08}$
This Study					
F10R30-N	26	15.9	15.9	1.6	1.6
F10R30-B2	27.3	48.2	39.3	0.6	0.7
F10R30-BU	32.3	49.3	40	0.6	0.8
F13R30-N	36.7	27.6	27.6	1.3	1.3
F13R30-B2	35.1	58.5	48.4	0.6	0.7
F13R30-BU	37.9	59.6	49.1	0.6	0.8
F16R0-N	50.3	42.3	42.3	1.2	1.2
F16R0-B2	50.4	71.1	59.4	0.7	0.8
F16R0-BU	53.7	72.2	59.9	0.7	0.9
F16R30-N	51.8	42.3	42.3	1.2	1.2
F16R30-B2	50.4	71.1	59.4	0.7	0.8
F16R30-BU	54.8	72.2	59.9	0.8	0.9
F16R30-LB2	53.6	73.3	60.4	0.7	0.9
F16R50-N	50.6	42.3	42.3	1.2	1.2
F16R50-B2	52.4	71.1	59.4	0.7	0.9
F16R50-BU	52.2	72.2	59.9	0.7	0.9
Average				0.9	0.9
Standard deviation				0.3	0.2
W.S. Kim et al. (2014)					
R0-13-N	34	30.2	31.9	1.1	1.1
R15-13-N	32.9	30.1	31.8	1.1	1
R30-13-N	31.2	29.9	31.8	1	1
R50-13-N	29.4	29.7	31.7	0.9	0.9
R15-13-S	43.1	30.1	42	1.4	1
R30-13-S	41.7	37	41.3	1.1	1
R50-13-S	37.9	36.2	40.5	1.1	0.9
R30-16-S	54.1	45.6	51.6	1.2	1.1
Average				1.1	1
Standard deviation				0.1	0.05
Attari et al. (2012)					
PA1	20.2	22.8	18.5	0.9	1.1
PA2	21.9	25.5	20.2	0.9	1.1
PA3	18.9	21.7	17.8	0.9	1.1
PB4	18.1	36.8	26.1	0.5	0.7
PB5	17.2	27.2	21.1	0.6	0.8
Average				0.7	0.9
Standard deviation				0.3	0.3

For LB2-serie of specimen, the sheet used for the BU-series test specimens was reinforced in two layers only at bottom side. Comparing with other specimens, the ultimate strength load was almost similar to that of the BU-series of specimens. On the other hand, the ductility of LB2-series of specimens showed an increase by 22.5% (Fig. 10). Bonding effect between para-aramid fiber sheets and concrete beams influenced effectively on flexural strengthening of the specimens through the experimental works in this study. In addition, the specimens strengthened by attaching fiber sheets to the bottom and sides demonstrated fewer crack patterns due to bridging effect of para-aramid fiber sheets Choi et al. (2011) (Table 9).

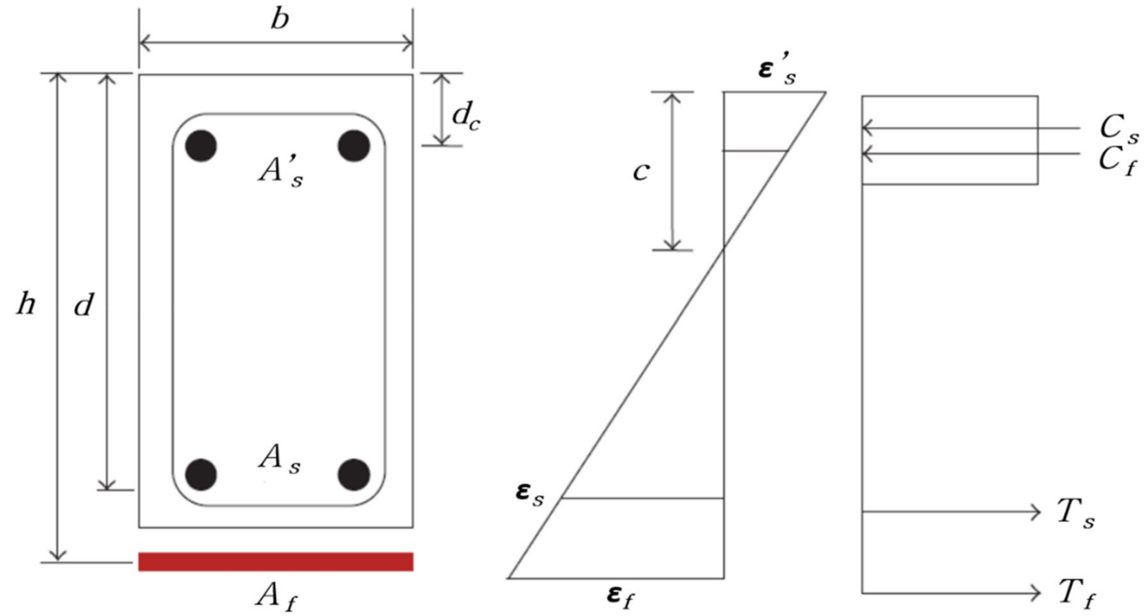

Fig. 11 The cross section and stress–strain diagram of beam

Figures illustrate that flexural capacity of RC beams without fiber reinforcement showed a decreasing progress when environmental-friendly recycled coarse aggregates replaced natural aggregates with ratio of 0%, 30% and 50% in concrete mix proportion. As a result, there was a decline in structural performance of the beams Malešev et al. (2010), McNeil et al. (2013). So, para-aramid fiber sheet reinforcement method was used to fix the loss in structural performance. Consequently, externally bonded FRP systems caused to strengthen the flexural characteristics of RC beams Yagar et al. (2022). Considering the measurements above, the effect of para-aramid fiber sheet reinforcement in EFRCA RC beams for flexural strength was effective through the experimental works in this study.

3.3 Verification and Comparison with Existing Structural Analysis Methods

According to ACI 440.2R-08., (2008) the nominal flexural strength in concrete beams with para-aramid FRP external reinforcement is computed using:

$$M_n = A_s f_y (d-) + \psi_f A_f f_f (h \frac{\beta_1 c}{2}) \tag{1}$$

where ψ_f is the reduction factor for FRP, c is the depth of concrete on compressive block; A_f is the cross section areas of FRP reinforcement; A_s are the cross section areas of tension rebar (Fig. 11).

Additionally, the method of Mahmoud T. El-Mihilmy addresses the flexural evaluations of reinforced concrete beams reinforced with externally bonded FRP Kim et al. 2014). A numerical method has been developed for the computation of the bending moment capacity of concrete beams with FRP reinforcement and the flexural failure mode predictions. The nominal flexural strength of the section with para-aramid FRP external reinforcement by El-Mihilmy is

$$M_n = A_s f_y (d-) + A_f f_f (d_f \frac{a}{2}) \tag{2}$$

where a is a depth of the equivalent rectangular concrete stress block; d is a depth to the centroid of the reinforcing steel A_s; d_f is a depth to the centroid of the FRP force; f_y is a yield strength of the reinforcing steel (Fig. 11).

To verify the results of the section analysis procedure, a comparison between the nominal flexural strength of the section with para-aramid FRP external reinforcement obtained experimentally, by the method of Mahmoud T. El-Mihilmy and Guide for the Design and Construction of Externally Bonded FRP Systems for Strengthening Concrete Structures reported by ACI Committee 440 (ACI 440.2R-08) ACI 440.2R-08., (2008), is presented. Table 5.2 summarizes the results of the comparison. From this Table, there is significant differences between the analytical calculations of the nominal flexural strength of the section with FRP external reinforcement obtained by the method of Mahmoud T. El-Mihilmy and ACI 440.2R-08. Predictions of the nominal flexural strength of the section externally reinforced with FRP by the method of Mahmoud T. El-Mihilmy showed higher

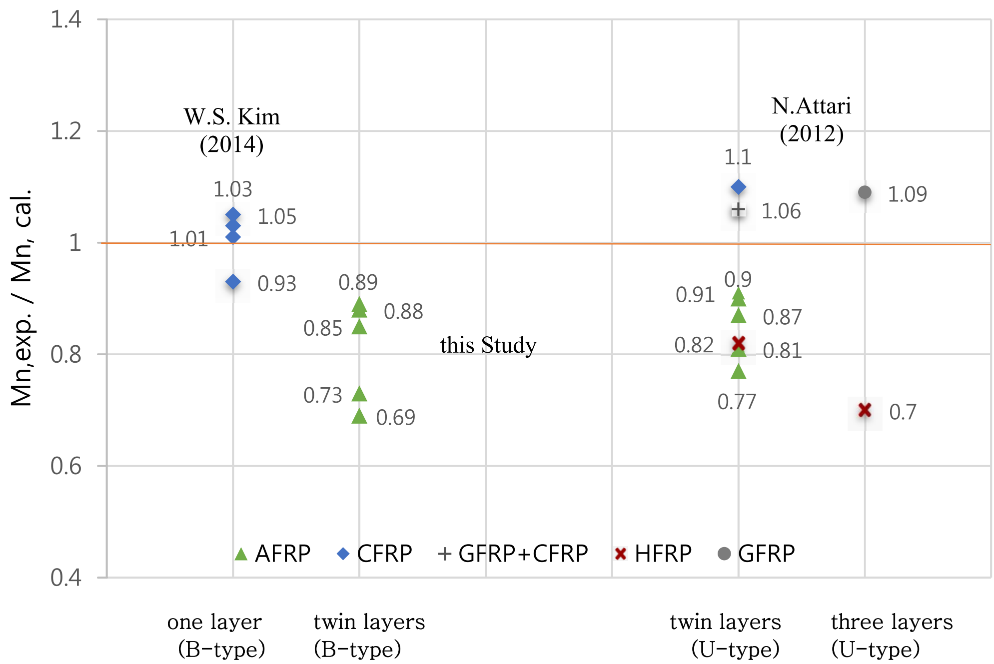

Fig. 12 A comparison between different experimental results of FRP strengthening (*AFRP* Aramid Fiber Reinforcement Polymer, *CFRP* Carbon Fiber Reinforcement Polymer Yang et al. (2007), *GFRP* Glass Fiber Reinforcement Polymer, *HFRP* Glass-Carbon Hybrid Fiber Reinforcement Polymer Wang and Zhou, (2018), *B-type* bottom part application, *U-type* bottom and side part application)

results than that of Guide for the Design and Construction of Externally Bonded FRP Systems for Strengthening Concrete Structures reported by ACI Committee 440. A difference between the results of these two structural analysis methods increased gradually as the tensile rebar size of specimens increased. When the experimental results were compared with the analytical predictions of the nominal flexural strength of the section with FRP external reinforcement, the measurements of the experimental study presented lower flexural characteristics. An average ratio between the test results and analytical predictions by the method of Mahmoud T. El- Mihilmy is 0.88. This ratio increases to 0.98 if to compare the experimental results with the results from the equation of ACI 440.2R-08. Among the experimental results, the nominal flexural strength of all specimens without para-aramid fiber sheet reinforcement showed higher flexural capacity than that of both analytical methods.

Fig. 12 shows the difference between some foreign and domestic experimental results on FRP reinforcement of RC beam comparing with this Research. A proportion of the nominal flexural strength of the section externally reinforced with FRP obtained experimentally and analytically, was taken to compare the difference of these studies. According to N. Attari et al. (2012), the use of a twin layer Glass-Carbon fibers composite material for strengthening reinforced concrete beams was very efficient. In the case of W.S. Kim et al. (2014), due to the high tensile strength of carbon fiber composite material significantly positive experimental results were obtained. From the Figure, it could be seen that the experimental specimen reinforced with Carbon Fiber Reinforcement Polymer from W.S. Kim et al. (2014) and the concrete beam strengthened with 2 layers of hybrid bidirectional glass-carbon Hybrid Fiber Reinforcement Polymer from N. Attari et al. (2012) presented the highest results when experimental results were higher than analytical calculations of the nominal flexural strength of the section externally reinforced with FRP. According to W.S. Kim et al. (2014), the most of all CRFP RC beams showed higher results than the expectations calculated by the method of Mahmoud T. El-Mihilmy and Guide for the Design and Construction of Externally Bonded FRP Systems for Strengthening Concrete Structures reported by ACI Committee 440 (ACI 440.2R-08).

4 Conclusions

Based on experimental observations and analysis results, the following conclusions were drawn:

(1) The BU-series specimens had fewer and narrower cracks before failure, indicating that the BU-type

aramid fiber sheet attachment method delivered loads more evenly.

(2) The BU-type attachment method for para-aramid fiber sheets is highly effective in strengthening reinforced concrete beams, with the 30% EFCRA ratio producing the best results.

(3) The F16R30-LB2 specimen showed the highest ductility when the type of aramid fiber sheet was changed from 4.5 mm interval to 14 mm interval.

(4) For N- and B2/LB2-series specimens, increasing the ratio of recycled aggregates improved flexural strength but decreased ductility. However, for BU-type reinforced specimens, flexural strength decreased as the ratio of recycled coarse aggregates increased.

(5) The F10R30-BU and F16R30-BU specimens had the highest ultimate loads, indicating the reinforcing effects of aramid fiber sheets.

(6) The nominal flexural strength of para-aramid FRP external reinforcement was lower than analytical predictions, but the ductile capacity of specimens showed that the reinforcement was effective for flexural strength in EFRCA RC beams.

Acknowledgements
Not applicable.

Author contributions
JR and WK conceived, designed and performed the experiments. WK supervised this project as a principal investigator. WK and JR analyzed the data and wrote the paper. All authors read and approved the final manuscript.

Funding
This work was supported by the National Research Foundation of Korea (NRF) grant funded by the Korea government (MSIT) (No. NRF-2017R1D1A3B03029863).

Availability of data and materials
The data presented in this study are available on request from the corresponding author.

Declarations

Competing interests
The authors declare that they have no competing interests.

Received: 5 October 2022 Accepted: 16 June 2023
Published online: 01 November 2023

References

ACI 440.2R-08. (2008). Guide for the design and construction of externally bonded FRP systems for strengthening concrete structures. ACI Committee 440, American Concrete Institute, Farmington Hills, MI, p. 76

Ahmadi, M., Farzin, S., Hassani, A., & Motamedi, M. (2017). Mechanical properties of the concrete containing recycled fibers and Aggregates. *Construction and Building Materials, 144*, 392–398.

Almusallam, T. H. (2006). Load-deflection behavior of RC beams strengthened with GFRP sheets subjected to different environmental conditions". *Cement & Concrete Composites, 28*, 879–889.

Arezoumandi, M., Smith, A., Volz, J., & Khayat, K. (2015). An experimental study on flexural strength of reinforced concrete beams with 100% recycled concrete aggregate. *Journal of Engineering Structures, 88*, 154–162.

Attari, N., Amziane, S., & Chemrouk, M. (2012). Flexural strengthening of concrete beams using CFRP, GFRP and hybrid FRP sheets. *Construction and Building Material, 37*, 746–757.

ACI Committee 318 (2008), Building Code Requirements for Structural Concrete and Commentary (ACI 318–08), American Concrete Institute, p. 456

Bai, W., & Sun, B. (2010). Experimental study on flexural behavior of recycled coarse aggregate concrete beam". *Applied Mechanics and Materials, 23–32*, 543–548.

Biswas, R., Sharma, N., & Singh, K. K. (2023). Numerical analysis of mechanical and fatigue behavior of glass and carbon fibre reinforced polymer composite. *Journal of Materials Today*. https://doi.org/10.1016/j.matpr.2023.03.479

Cho, Y., Jang, H., Back, S., Choi, M., Hong, S., & Lee, Y. (2016). Evaluation of sustainable structural concrete using recycled aggregate and aramid fiber sheet. *Advances in Materials Science and Engineering*. https://doi.org/10.1155/2016/2721859

Choi, D., Kang, T.H.-K., Ha, S., Kim, K., & Kim, W. (2011). Flexural and bond behavior of concrete beams strengthened with hybrid carbon-glass fiber-reinforced polymer sheets. *ACI Structural Journal, 108*(1), 90–98.

Etxeberria, M., Vázquez, E., Mari, A., & Barra, M. (2007). Influence of amount of recycled coarse aggregates and production process on properties of recycled aggregate concrete". *Cement and Concrete Research, 37*(5), 735–742.

Garcez, M., Meneghetti, L., & da Silva, F. L. (2008). Structural performance of RC beams poststrengthened with carbon, aramid, and glass FRP systems. *Journal of Composites for Construction, 12*(5), 522–530.

Guo, R., Li, C., Niu, Y., & Xian, G. (2022). The fatigue performances carbon fiber reinforced polymer composites – A review. *Journal of Materials Research and Technology*, 4773–4789.https://doi.org/10.1016/j.matpr.2021.11.053.

Kim, W. (2011). Experimental analysis for steel congestion relief in concrete structures under monotonic and seismic loads. Ph.D. dissertation, University of Oklahoma, Norman, OK, USA.

Kim, H. (2012). Experimental studies of effect of beam sizes and CFRP layers on structural behaviors of reinforced concrete beams strengthened with CFRPs (Carbon fiber reinforced polymers)". *Journal of the Architectural Institute of Korea Structure & Construction, 28*(11), 99–106.

Kim, J., Baek, S., Kim, W., & Kwak, Y. (2012). A study on the behavior reinforced concrete beam-column joints made with recycled aggregate under cyclic loading". *Journal of the Architectural Institute of Korea Structure & Construction, 28*(7), 9–30.

Kim, W., Kang, T.H.-K., Lee, D., Choi, H., & Kwak, Y. (2020). Shear strength of reinforced concrete beams using recycled coarse aggregates without stirrups. *ACI Structural Journal, 117*(6), 281–295.

Kim, W., & Kwak, Y. (2015). A case study of the performance evaluation for recycled aggregate concrete strengthened with advance composite fibers. *Journal of the Korean Society for Advanced Composite Structures, 6*(2), 31–39.

Kim, W., Park, H., Kim, B., Baek, S., & Kwak, Y. (2014). Experimental study on the flexural strengthening effect of recycled coarse aggregate RC beams strengthened with carbon fiber reinforced polymers. *Journal of the Architectural Institute of Korea Structure & Construction, 30*(7), 3–12.

Lee, H., Kim, S., Lee, H., Azimov, E., & Kim, W. (2018). A study on the mechanical properties of para-aramid fiber-reinforced concrete using environment-friendly recycled coarse aggregates. *Journal of the Korean Society for Advanced Composite Structures., 9*(1), 62–71.

Lee, H., Koo, E., & Lee, L. (1998). An experimental study of flexural behaviors of the RC beams strengthened by carbon sheets". *Journal of the Architectural Institute of Korea Structure & Construction, 14*(6), 77–84.

Lu, Z., Li, J., Xie, J., Huang, P., & Xue, L. (2021). Durability of flexurally strengthened RC beams with prestressed CFRP sheet under wet–dry cycling in a chloride-containing environment. *Composite Structures, 255*(2021), 112869.

Malešev, M., Radonjanin, V., & Marinkovi, S. (2010). Recycled concrete as aggregate for structural concrete production. *Journal of Sustainability, 2*, 1204–1225.
McNeil, K., & Kang, T.H.-K. (2013). Recycled concrete aggregates: a review. *International Journal of Concrete Structures and Materials, 7*(1), 61–69.
Ortiz, J. D., Dolati, S. S. K., Malla, P., Nanni, A., & Mehrabi, A. (2023). FRP-Reinforced/Strengthened concrete: State-of-the-art review on durability and mechanical effects. *MDPI Materials*. https://doi.org/10.3390/ma16051990
Qureshi, J. (2022). A review of fibre reinforced polymer structures. *MDPI. Fibers*. https://doi.org/10.3390/fib10030027
Rao, A., Jha, K., & Misra, S. (2007). Use of aggregates from recycled construction and demolition waste in concrete". *Journal of Resources, Conservation and Recycling, 50*, 71–81.
Saleem, M. U., Qureshi, H. J., Amin, M. N., Khan, K., & Khurshid, H. (2019). Cracking behavior of RC beams strengthened with different amounts and layouts of CFRP. *Journal of Applied Sciences, 9*, 1017.
Sato, R., Maruyama, I., Sogabe, T., & Soga, M. (2007). Flexural behavior of reinforced recycled concrete beams. *Journal of Advanced Concrete Technology, 5*(1), 43–61.
Tatar, J., & Milev, S. (2021). Durability of externally bonded fiber-reinforced composites in concrete structures: a critical review. *MDPI Polymers*. https://doi.org/10.3390/polym13050765
Wang, X., & Zhou, C. (2018). Numerical investigation for the flexural strengthening of reinforced concrete beams with external prestressed HFRP sheets. *Construction and Building Materials, 189*, 804–815.
Yagar, A. C., Inche, C., & Derogar, S. (2022). FRP Strengthening of RC structures: sustainable, environmental and structural evaluations. *Journal of Sustainable Construction Materials and Technologies, 7*(4), 358–374. https://doi.org/10.47481/jscmt.1211086
Yang, D., Park, J., You, Y., & Park, S. (2007). Flexural behavior and analysis of RC beams strengthened with prestressed CFRP plates. *Journal of Korea Concrete Institute, 19*(4), 467–474. https://doi.org/10.4334/JKCI.2007.19.4.467
Yang, I., & Jeong, J. (2016). Effect of recycled coarse aggregate on compressive strength and mechanical properties of concrete". *Journal of the Korea Concrete Institute, 9*(4), 131–137.
Yoo, S., Yuan, T., Hong, S., & Yoon, Y. (2020). Evaluation of structural performance of concrete beams strengthened with carbon fiber sheets and no-slump concrete. *Journal of Korean Society of Hazard Mitigation, 20*(4), 185–193. https://doi.org/10.9798/KOSHAM.2020.20.4.185

Publisher's Note

Jamshid Ruziev is a Ph.D. Student in the Department of Architectural Engineering at the Kumoh National Institute of Technology, 61 Daehak-ro, Gumi, Gyeongsangbuk-do 39177, Republic of Korea.

Woosuk Kim is an Associate Professor in the School of Architecture at the Kumoh National Institute of Technology, 61 Daehak-ro, Gumi, Gyeongsangbuk-do 39177, Republic of Korea.